

# Load-deflection of a low-stress SiN-membrane/Si-frame composite diaphragm

J. H. Correia, M. Bartek and R. F. Wolffenbuttel

**Abstract**--Finite-Element-Methods (FEM) has been used to study the behavior of a non-planar composite diaphragm, which is to be used in a tunable Fabry-Perot-based silicon microinterferometer. The composite (Ag-mirror/low-stress SiN membrane/Si-frame) diaphragm used exhibits: excellent flatness, high mechanical strength for large and thin structures, good optical properties and low-voltage electrostatic actuation. Moreover, FEM simulations show that highest stress occurs at the middle of the four outer edges of the diaphragm and maximum stress levels are below the fracture limit of the membrane. The load-deflection behavior of the (membrane/Si-frame) composite diaphragm is presented. The analysis takes into account the shape of the frame and that of the electrodes. The influence of the frame convex corner overetch on the stress profile was also investigated. Results from FEM simulations were subsequently confirmed experimentally. Surface profilometer measurements were used to verify the load-deflection behavior of the diaphragm. The resulting error is less than 10%. This work is restricted to square diaphragms, which can be fabricated using simple bulk-micromachining.

**Index Terms**--load-deflection, diaphragms, silicon nitride membrane, Fabry-Perot microinterferometer, LPCVD silicon nitride, residual stress, high flatness, strain.

## I. INTRODUCTION

High performance diaphragm structures are not only very important in MEMS applications (e.g. pressure sensors, microphones and accelerometers), but also in micro-opto-electro-mechanical devices. Thin electrostatically driven diaphragm-mirrors have been used for imaging applications, because of their high stability at small deflections. Also, adaptive mirrors based on large area silicon nitride diaphragms were applied for correction of optical aberrations in real time [1].

To avoid expensive “trial and error” process runs, it is important to be able to predict the mechanical behavior of the diaphragm as well to optimize its design according to application requirements. The load-deflection function of silicon diaphragms can be predicted using simple calculations based on approximate analytical methods. But, these lack the ability to deal with corrugation profiles, complex shapes, effects arising from internal stress and stress discontinuities. Therefore, use of finite element methods becomes necessary in modeling and simulating more complex diaphragms.

The authors are with the Lab. for Electronic Instrumentation/Dimes, ITS-Dept. of Electrical Engineering, Delft University of Technology, Mekelweg 4, 2628 CD Delft, The Netherlands.

The mechanical behavior of diaphragms is governed mainly by their geometry (thickness, shape) and material properties (residual built-in stress, Young’s modulus, Poisson ratio). The material data depends strongly on the fabrication process conditions. Therefore, for accurate results, reliable data extracted for a particular process is required.

In this paper the load-deflection behavior of a composite diaphragm (Ag-mirror/SiN-membrane/Si-frame), which is to be used in a Fabry-Perot microinterferometer, has been studied.

## II. DIAPHRAGM DESIGN

### A. Fabry-Perot microinterferometer requirements

A Fabry-Perot microinterferometer (schematically shown in Fig. 1) consists of a vertically integrated structure composed of two mirrors separated by an air gap (optical resonance cavity). One of the mirrors is fixed, the other is deflected (for instance electrostatically) for wavelength tuning. Successful operation of a tunable Fabry-Perot device requires: parallelism of the mirrors, flatness and stability in the optically active region, low tuning voltage and good optical properties (mirrors with high reflectivity and low absorption). Therefore, the diaphragm must feature high transparency in the wavelengths region required, flatness over the entire region of operation, elasticity and high mechanical strength to allow fabrication of large and thin structures.

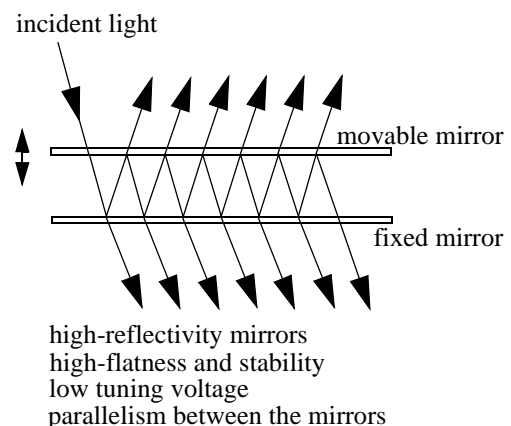


Fig. 1: Fabry-Perot microinterferometer requirements.

The deflection required is typically between 300 nm to 2  $\mu\text{m}$  (for operation over the entire visible spectral range) for optical cavities with a cavity gap spacing between 1  $\mu\text{m}$  to 6  $\mu\text{m}$  respectively. The optical aperture range simulated is from 100x100  $\mu\text{m}^2$  up to 2x2  $\text{mm}^2$ .

### B. Selection of the diaphragm geometry

The possible types of the diaphragm considered are: (a) cantilever [2], (b) "H"-shaped structure (square suspended membrane with four beams), (c) simple clamped membrane, (d) perforated membrane, (e) composite  $\text{SiO}_2/\text{SiN}$  diaphragm [3], (f) silicon nitride membrane/silicon frame (see Fig. 2).

FEM simulations show that the cantilever (a) needs relatively low tuning voltage to bend, but flatness and parallelism deteriorates with increased deflection. This observation is in agreement with literature [2]. Therefore, conditions for optical resonance will be achieved only in a very small region, which strongly limits the application in a Fabry-Perot device. Simple fabrication using bulk or surface micromachining is one of the advantages of this structure. The square suspended membrane with four beams (b) needs a higher voltage for an equivalent bending as in (a), but the area over which it can be considered flat is not improved much. The simple clamped membrane (c) shows the highest voltage required to bend compared to (a) and (b). The area over which the deflected membrane can be regarded as flat is larger, but far from ideal (see Fig. 3). In the case of the perforated membrane (d) the etch holes reduce the effect of the membrane internal stress (also leads to a reduction of the squeezed-film damping). Consequently, structure (d) features a reduced tuning voltage, but the flat area is not better than in (c) [4][5]. The composite  $\text{SiO}_2/\text{SiN}$  diaphragm (e) takes advantage from the compressive stress in  $\text{SiO}_2$  films to compensate for the silicon nitride tensile stress, in order to reduce the internal stress [3]. The fabrication process of the structures (d) and (e) is more complex than the others.

The composite (silicon nitride membrane/silicon frame) diaphragm (f), requires the highest voltage for deflection compared to all other structures. However, the silicon frame ensures a flatness over a large area (Fig. 4). The silicon frame is used instead of a "mesa", because the inner part of the frame is used as active region of the Fabry-Perot device. The fabrication process is simple and comparable with structure (c).

Corrugated silicon membranes exhibit large and linear deflection [6], however compressive stresses generated in such regions originates membrane buckling. Therefore, corrugated structures were avoided in the diaphragm geometry study.

From all the diaphragm structures considered, FEM simulations show that the mechanical and optical behavior

of the structure (f) is closest to the requirements of intended application (see Table 1). Also, the fabrication of this type of diaphragm promises a relatively simple high-yield process.

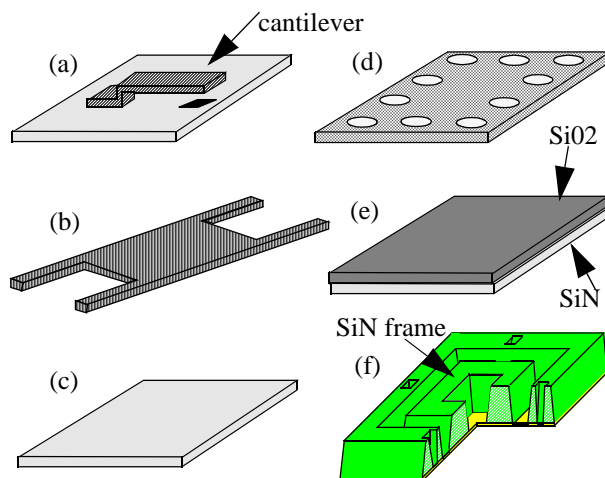


Fig. 2: Diaphragm structures: (a)-cantilever, (b)-"H" shaped structure held in on four sides, (c)-simple membrane, (d)-perforated membrane, (e)-composite  $\text{SiO}_2/\text{SiN}$ , (f)- $\text{SiN}$ -membrane/ $\text{Si}$ -frame.

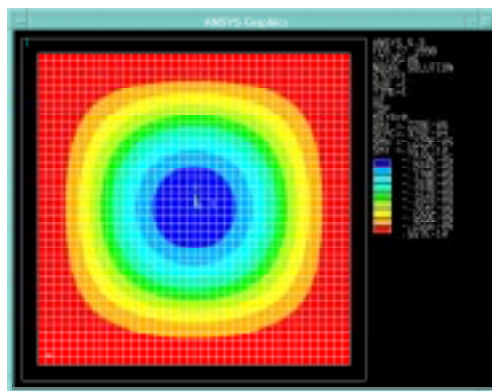


Fig. 3: Deflection of a membrane without frame (structure c).

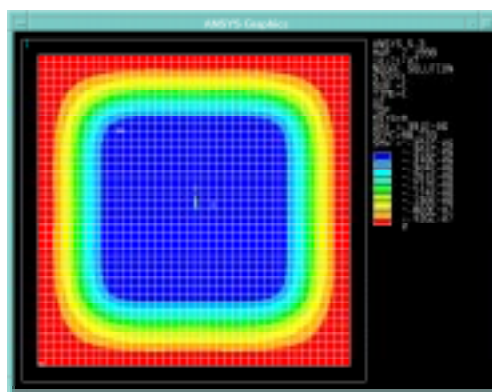


Fig. 4: Deflection of a membrane with frame (structure f).

Table 1: Advantages/drawbacks of different structure types

Structure type simulated	Fabric.	Low Voltage	Internal stress	Flatness
cantilever (a)	-	++	+	--
“H”-shaped (b)	-	+	+	--
membrane <sup>1</sup> (c)	0	0	0	0
perf. memb. (d)	-	+	+	-
SiO <sub>2</sub> /SiN (e)	-	+	+	0
Si-frame/SiN (f)	0	-	0	++

<sup>1</sup>Simple membrane is used as reference

### C. Diaphragm materials and fabrication

Several materials have been considered for diaphragm fabrication: silicon, silicon nitride, oxynitride. Silicon nitride has been used in combination with bulk micromachining, as its mechanical strength and the high SiN/Si etch selectivity in KOH allows the fabrication of large and thin membranes. Also, silicon nitride is transparent in the visible optical range and has been applied to micro-optical devices, such as microinterferometers, despite the fact that control is required to avoid excessive stress levels. The internal stress in silicon nitride membranes is determined by the deposition conditions and annealing temperature [7].

Square diaphragms (SiN-membrane/Si-frame) were fabricated using KOH anisotropic etching from the backside of the wafer in a 33wt% KOH solution (85°C), using the low-stress LPCVD silicon nitride on the backside as an etch mask. The same silicon nitride layer is used on the front side as a deformable membrane. The mirror was formed by evaporation of a thin silver layer (40 nm) on the SiN-membrane. The tensile stress in the thin silver layer based mirror is very low compared to the SiN-membrane tensile stress and therefore, was neglected in this study.

## III. DIAPHRAGM SIMULATIONS

### A. Input data

The input data for FEM simulations are the optical constraints and material properties (Young’s modulus-E, internal stress- $\sigma$ , Poisson’s ratio- $\nu$ ). We recognize that for a given structure, a higher-performance load-deflection characteristic can be obtained using a circular membrane. However, this work is restricted to square diaphragms, which can be fabricated using simple bulk-micromachining. Different diaphragm lateral dimensions (typically between 3x3 mm<sup>2</sup> and 8x8 mm<sup>2</sup>), membrane thicknesses (from

150 nm to 1  $\mu$ m), frame sizes (from 1.8x1.8 mm<sup>2</sup> to 4x4 mm<sup>2</sup>) and square apertures dimensions (between 200  $\mu$ m to 2 mm) were simulated. These values are mostly set by technology constraints (Fig. 5). The etching of silicon in KOH is very anisotropic: the {100} planes and {110} planes are selectively etched, while the etch-rate in the <111> direction is much lower [8]. As a result, when etching a square membrane in a (100)-cut wafer (thickness 525  $\mu$ m) in KOH, side-walls are formed under an angle of 54.74° with respect to the surface. A top frame width of 50  $\mu$ m, thus implies a bottom frame width (and also a backside mask pattern) of 794  $\mu$ m. Also, the frame convex corners will be etched away, resulting in a loss of the desired structure [9]. To prevent this, corner compensation structures have been added at the convex corners of the silicon frame.

The values used in FEM simulations (see Fig. 6) for low stress LPCVD silicon nitride were: E=360 GPa,  $\sigma$ =0.125 GPa (material data extracted from the fabrication process used) [7].

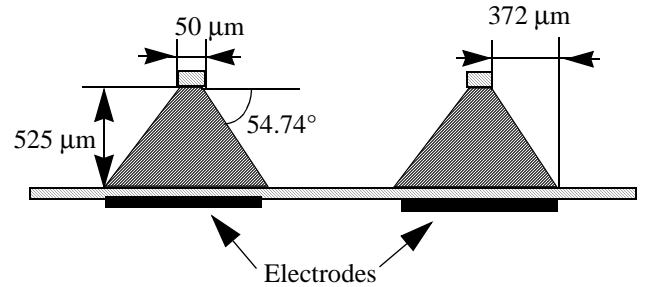


Fig. 5: Dimensions set by technology constraints.

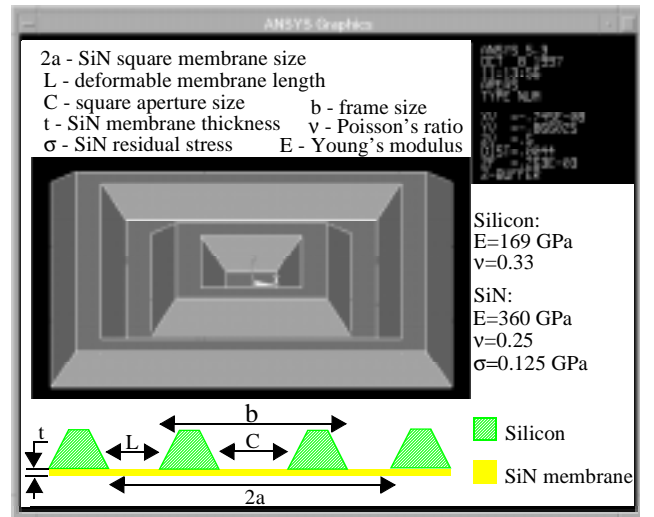


Fig. 6: Input data for the FEM simulations of composite diaphragm.

### B. FEM techniques

To model a device using FEM it is necessary to define [10]: the type of construction elements, mesh profile, material properties, boundary conditions and loads. The conditions and requirements relevant in the FEM simulation of the diaphragm are:

1. the top-plate is initially flat, parallel and movable with respect to the bottom-plate (fixed infinite ground plate).
2. the movable plate operates in the small-deflection regime until pull-in occurs (linear elastic mechanics).
3. the movable plate has perfect boundary conditions (all six degrees of freedom at each boundary are fixed).

Diaphragm thickness, dimensions and the load-deflection behavior were optimized with FEM in order to achieve large deflection at a minimum value of the electrostatic control voltage.

The membrane was modeled by a three-dimensional shell element (very small thickness) and the silicon frame by a three-dimensional solid. A mesh refinement at the corner regions of both diaphragm and frame improves precision of the FEM simulations. The membrane residual tensile stress was simulated by defining a thermal-expansion coefficient and applying a temperature load.

### C. Load-deflection analysis

Tabata *et al.* [11] [12] presented an analytical solution for load-deflection of rectangular flat membranes:

$$P = \frac{C_1 t \sigma d}{a^2} + \frac{C_2 t E d^3}{a^4} \quad (1)$$

where P denotes the applied pressure, d the center deflection, a one half of the membrane's edge length, t the membrane thickness,  $\sigma$  the residual stress, E the Young's modulus,  $c_1=3.04$  and  $c_2=1.83$ .

The first term indicates the stiffness that is governed by the residual stress of the membrane and the second term presents the stiffness of the material. Pan *et al.* [13] have found values  $c_1=3.41$  and  $c_2=2.45$  using FEM analysis. These calculations were carried out for membrane deflection  $d \gg t$ .

Our structure has a silicon frame (with irregular shape) on the membrane. The load to deflect the diaphragm is applied only at the area under the frame (localized pressure due to voltage applied at control electrodes), defined by its bottom width and length dimensions. Therefore, in order to understand the mechanical behavior of this device (analytical treatment is only valid for rough estimations), numerical calculations based on FEM must be used.

FEM simulations were used to study the influence of the deformable length L and the frame size b for the deflection of the diaphragm (Fig. 7 and Fig. 8). For small deflections (less than 2  $\mu\text{m}$ ) the deflection is directly proportional to L and inversely proportional to b.

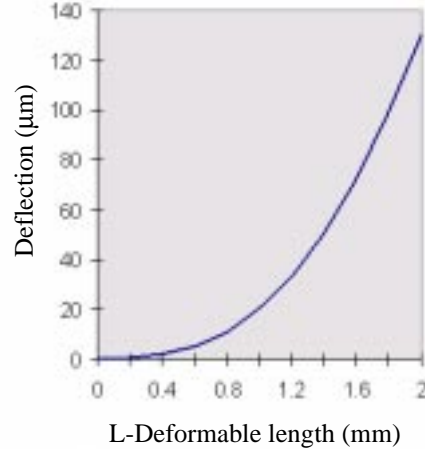


Fig. 7: Deflection for different values of L when the force applied and the frame size are constant.

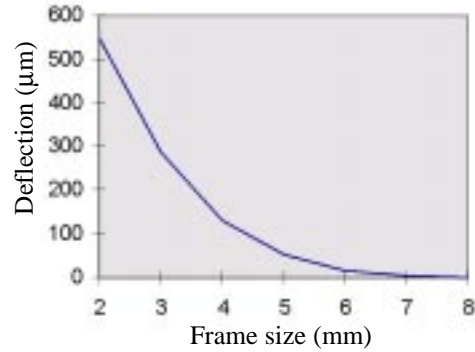


Fig. 8: Frame deflection for different values of b (frame size) when the force applied and the diaphragm size are constant.

### D. Influence of internal stress

A flexible membrane preserves its shape in case of lateral tension. This is the main reason to choose silicon nitride for the membrane material. Tensile stress membranes improve the flatness and optical quality. However, an increasing tensile stress requires an increasing voltage for electrostatic actuation. Therefore, a compromise between voltage and built-in internal stress is required. The deposition conditions of the LPCVD silicon nitride as well the annealing temperature used allows setting of the internal built-in stress at a suitable value equal to 0.125 GPa.

### E. Influence of corner shape

Bulk micromachining could influence the corner shape, which may affect:

1. the deflection of the center of the diaphragm
2. the stress concentration in the corner.

Typically, a sharp corner geometry gives rise to the stress concentration. For this reason, small variations in the shape of the corner when etched can have a dramatic influence on the device behavior. To avoid overetching of the frame convex corners during the anisotropic etching of silicon, corner compensation structures were used. Fig. 9 shows a typical corner shape when compensation structures were used.

The corner overetching depends on the etching time and this parameter can therefore be used to control the resulting corner shape. An example of a corner with different etching ratios was simulated in order to study the deflection of the diaphragm with a constant force applied (see Fig. 10). The results show a deflection four times higher at the same force applied in case of a 50% corner overetch (overetching defined as indicated in insert in Fig. 10). Therefore, selective overetching can be used to decrease the value of the electrostatic voltage necessary for deflection.

The stress concentration difference for a same deflection (until  $2 \mu\text{m}$ ) in an 100% overetched corner and a perfect corner is not significant (less than 1 MPa at 127 MPa). However, for large deflections (high loads), very high values of stress concentration can be encountered, especially in thin membranes.

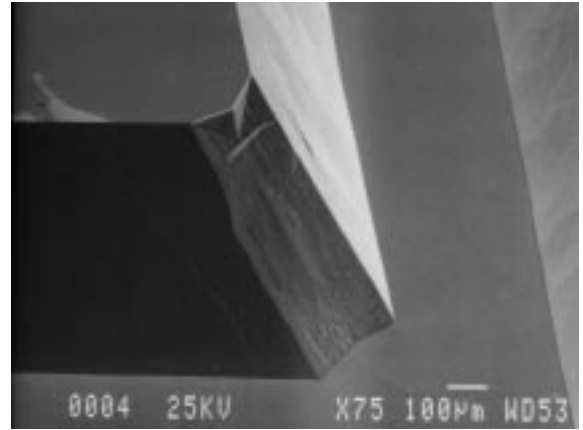


Fig. 9: Etching of (100)-oriented corner compensation structures in aqueous KOH with resulting convex corner [9].

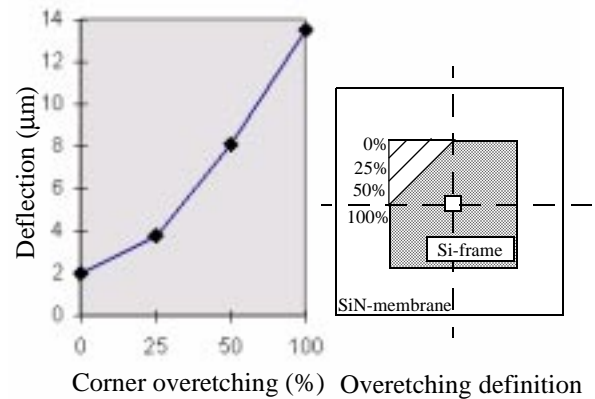


Fig. 10: Deflection achieved for different corner overetching.

## IV. EXPERIMENTAL RESULTS

To test the diaphragms load-deflection behavior, a TENCOR Alpha-Step 500 surface profilometer with a needle force of  $187 \mu\text{N}$  and a vertical resolution of 2.5 nm was used.

The surface profilometer scan across the entire membrane (this corresponds to the deformable membrane area, frame area and mirror surface) is shown in Fig. 11. The scanning length was 4.2 mm, corresponding to the active area of the diaphragm (edge to edge).

The data obtained was compared with the FEM simulations for the same conditions (frame size 3.0 mm, deformable membrane length 0.6 mm and mirror square aperture 1.2 mm). The results show that low-stress non-planar composite diaphragms can be simulated within 10% of error. If we correct for the errors associated with the measurement of the diaphragm thickness and internal residual stress, the error will be reduced.

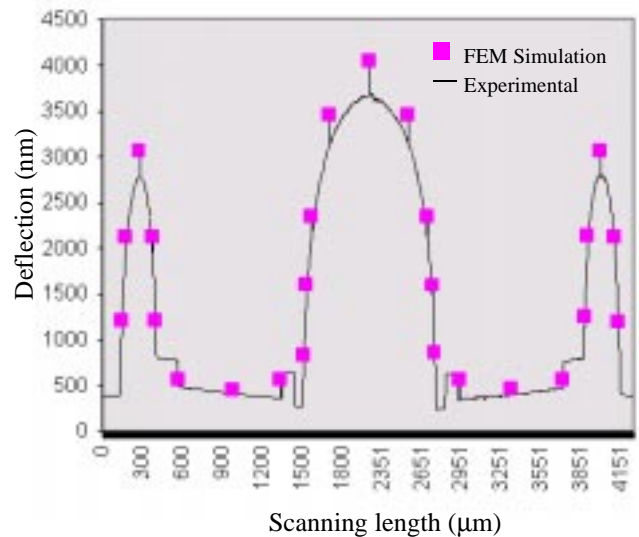


Fig. 11: Comparison of a surface profilometer scan (needle force of  $187 \mu\text{N}$ ) with FEM simulations.

A photograph of the fabricated tunable Fabry-Perot microinterferometer, with one of the mirrors based on the diaphragm studied in previous sections, is shown in Fig. 12.

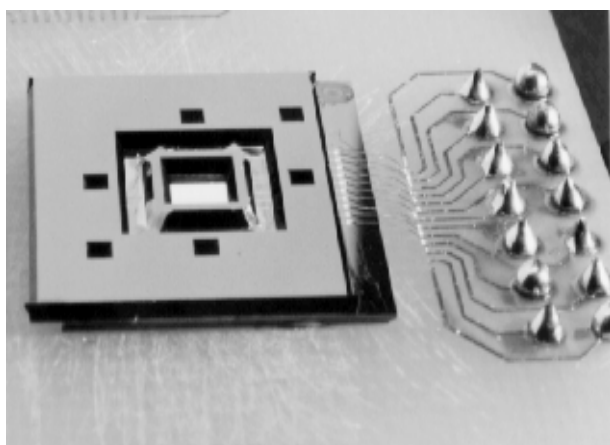


Fig. 12: Photograph of the fabricated Fabry-Perot microinterferometer with upper mirror based on simulated composite diaphragm.

## V. CONCLUSIONS

Composite diaphragms (SiN-membrane/Si frame) have been fabricated and their load-deflection performance was measured and compared with FEM simulations. The error achieved is less than 10%. Therefore, FEM simulations are reasonably reliable for providing theoretical insight into the complex device behavior and its operation. The main results achieved by FEM simulations and subsequently confirmed experimentally are:

1. SiN-membrane/Si-frame diaphragm presents the highest performance for our optical application
2. excellent flatness in the frame region
3. highest stress occurs at the middle of the four outer edges of the diaphragm
4. maximum diaphragm stress below fracture stress of the membrane (2 GPa)
5. overetching of the frame convex corners can be used to decrease the voltage required for a certain frame deflection.

An issue that requires further study is the effect of an increase of the stress due to wafer bonding or die attachment for the complete Fabry-Perot microinterferometer device. Also, the limits of the tilt control to achieve parallelism of the mirrors in the F-P device are under investigation.

## ACKNOWLEDGMENTS

The authors would like to thank the staff of Delft Institute of Microelectronics and Submicron Technology (DIMES), especially J. Groenweg, for technical assistance in fabrication of the devices. This work is supported in part by STW (project DEL 55.3733), TUDelft and JNICT-Portugal (Program Praxis XXI-BD/5181/95).

## REFERENCES

- [1] G. Vdovin, P.M. Sarro, "Flexible mirror micromachined in silicon", *Applied Optics*, 34, pp. 2968-2972, 1995.
- [2] J. D. Patterson, B. van Zeghbroeck, "Fabrication and analysis of Si/SiO<sub>2</sub> micromechanical modulators", *Digest IEEE-LEOS 1996 Summer topical meeting on optical MEMS and their applications*, pp. 25-26, USA, 1996.
- [3] S. Vergote, M. Cooman, P. Wouters, B. Puers, "A composite membrane movement detector with dedicated interface electronics for animal activity tracking", *Sensors and Actuators A*, 37-38, pp. 86-90, 1993.
- [4] V. L. Rabinovich, R. K. Gupta, S. D. Senturia, "The effect of release-etch holes on the electromechanical behavior of MEMS structures, *Proc. of Transducers'97*, pp. 1125-1128, Chicago, USA, June 1997.
- [5] Y. Yang, M. Gretillat, S. D. Senturia, "Effect of air damping on the dynamics of nonuniform deformations of microstructures", *Proc. of Transducers'97*, pp. 1093-1096, Chicago, USA, June 1997.
- [6] Y. Zhang, K. D. Wise, "Performance of Non-Planar Silicon Diaphragms under Large Deflections", *JMEMS* Vol. 3, No.2, pp.59-68, June 1994.
- [7] P. J. French, P.M.Sarro, R. Mallee, E.J.M. Fakkeldij, R. F. Wolffenbuttel, "Optimization of a low-stress silicon nitride process for surface-micromachining applications", *Sensors and Actuators A*, 58, pp.149-157, Feb. 1997.
- [8] H. Seidl, L. Csepregi, A. Heuberger and H. Baumgartel, "Anisotropic etching of crystalline silicon in alkaline solutions, orientation dependence and behavior of passivation layers", *J. Electrochemical Society*, vol. 137, pp. 3612-3626, 1990.
- [9] R. P. van Kampen and R. F. Wolffenbuttel, "Effects of <110>-oriented corner compensation structures on membrane quality and convex corner integrity in (100)-silicon using aqueous KOH, *J. Micromech. Microeng.*, 5, pp.91-94, 1995.
- [10] S. D. Senturia, Narayan Aluru, J. White, "Simulating the Behavior of MEMS Devices: Computational Methods and Needs", *IEEE Computational Science & Engineering*, pp. 30-43, March 1997.
- [11] O. Tabata, K. Kawahata, S. Sugiyama, I. Igarashi, "Mechanical property measurements of thin films using load-deflection of composite rectangular membranes", *Sensors and Actuators A*, 20, pp. 135-141, 1989.
- [12] S. Timoshenko, S. Woinowsky-Krieger, "Theory of plates and shells", McGraw-Hill, New York, NY, USA, 1959.
- [13] J. Y. Pan, P. Lin, F. Maseeh, S. D. Senturia, "Verification of FEM analysis of load-deflection methods for measuring mechanical properties of thin films" in *Tech. Dig. IEEE Solid-State Sensors and Actuators Workshop*, Hilton Head Island, SC, USA, pp. 70-73, 1990.